Optogenetic activation of dorsal raphe serotonin neurons induces a brain-wide response in reward network

Hiro Taiyo Hamada[1,3,*], Yoshifumi Abe[2], Norio Takata[2], Masakazu Taira[1], Kenji F. Tanaka[2], Kenji Doya[1,*]

[1] Neural Computation Unit, Okinawa Institute of Science and Technology Graduate University, Okinawa, Japan

[2] Department of Neuropsychiatry, Keio University School of Medicine, Tokyo, Japan

[3] Research & Development Department, Araya Inc., Tokyo, Japan

* Correspondence to hamada_h@araya.org, doya@oist.jp

Abstract

Serotonin is a neuromodulator that affects multiple behavioral and cognitive functions. Nonetheless, how serotonin causes such a variety of effects through its brain-wide projections and variety of receptors remains unclear. Here we measured the brain-wide response to optogenetic stimulation of serotonin neurons in the dorsal raphe nucleus (DRN) by functional MRI using an 11.7T scanner with a cryoprobe. Transient activation of DRN serotonin neurons caused wide-spread activation of reward-related brain areas. The same stimulation under anesthesia with isoflurane decreased activation of those reward-related areas and the hippocampal complex. These brain-wide response patterns can be explained by DRN serotonergic projection topography and serotonin receptor expression profiles, with enhanced weights on 5-HT1 type receptors. The primarily facilitatory effect on reward-related brain areas by DRN serotonergic activation is consistent with recent discoveries of its roles in reward-oriented behaviors and demands reconsideration of inhibitory view due to the result under anesthesia.

Introduction

Serotonin, 5-hydroxytryptamine (5-HT), serves crucial behavioral and cognitive functions, including awake-sleep cycle, mood, reward and punishment predictions [3,20], patience [24,25], and learning [12]. Serotonin is also a major target of medications for psychiatric disorders, notably major depression, by selective serotonin re-uptake inhibitors (SSRIs). The dorsal raphe nucleus (DRN) is a major source of serotonergic projections to brain-wide targets, including the frontal cortex, the basal ganglia, the ventral tegmental area (VTA), and other mid-brain regions [30]. DRN contains glutamatergic, GABAergic, and dopaminergic neurons in addition to serotonergic neurons [7]. Optogenetic manipulation of serotonin neuron activities has revealed their roles in reward [15,16], patience [24,25], anxiety [18,28], and learning [12,27]. How brain-wide serotonergic projections cause such effects, and by which target areas and receptors, however, remains only partially understood through optogenetic stimulation of serotonergic axon terminals [23,40].

In order to clarify the global picture of serotonergic control of brain-wide networks, we performed optogenetic functional MRI experiments using Tph2-ChR2(C128S) transgenic mice and an 11.7T MRI scanner with a cryoprobe for high S/N measurement. A previous optogenetic fMRI experiment activated DRN serotonin neurons using the Pet1 promoter under anesthesia and showed widespread suppression of cortical activities [9]. We introduced an acclimation protocol to allow stable fMRI recording from awake mice [1,42] and found that DRN serotonin activation in an awake state induced a brain-wide activity increase in reward-related areas, both in the cortical and subcortical areas. In contrast, under anesthesia with isoflurane, DRN serotonin activation decreased activities in those areas, consistent with a previous study [9].

We further revealed that regional BOLD responses can be approximated by a linear model with projection densities of DRN serotonin neurons and expression profiles of different types of serotonin receptors, with negative coefficients for 5-HT1 type receptors and positive coefficients for 5-HT2 type receptors. These results suggest that serotonergic neurons activate reward-related circuits and they demand reconsideration of the implications of results under anesthesia.

Results

In order to clarify the effect of the brain-wide serotonergic projections, we employed optogenetic fMRI combining optogenetic stimulation of serotonergic neurons in the dorsal raphe nucleus (DRN) and measurements of whole-brain activities by functional

MRI. We used Tph2-ChR2(C128S) transgenic mice [28,34] which express step-type channel rhodopsin selectively in serotonin neurons [25,28]. We used an 11.7T MRI scanner (Bruker BioSpec 117/11) with a cryoprobe for high S/N recording of BOLD signals from the whole brain, except the olfactory bulb and the posterior cerebellum.

Prior to experiments, the transgenic and wild-type (WT) groups (Transgenic group: n = 8; Wild-type: n = 6) underwent surgery to attach a plastic fixation bar and implant an optical cannula in the DRN. Acclimation training in a mock chamber followed (Figure 1. See Methods for details). After the fMRI experiments, animals were tested in a reward waiting task [24,25] to confirm the effectiveness of optogenetic stimulation (Supplementary Figure S1).

DRN Serotonin activation induces a brain-wide increase in the BOLD signal

We measured BOLD responses under optogenetic stimulation of DRN serotonin neurons in an ON/OFF block design protocol (Figure 1.e). Photo-stimulation increased the BOLD signal in DRN (Figure 1.f), with a tendency for reduced response after repeated stimulation. On average, over five stimulations, blue light stimulation induced a significantly higher BOLD response than did yellow light stimulation ($p < 0.05$, multiple-correction; Figure 1.f).

A group analysis with a general linear model (GLM) of photo-activated BOLD responses between transgenic (n = 8) and WT mice (n = 6) revealed a brain-wide increase in BOLD responses, significantly in the frontal cortex, the caudate putamen (CPu), the temporal cortical regions, the thalamic complex, and the VTA ($p<0.05$, cluster-wise correction; Figure 2.a). Trial-wise BOLD responses also showed a consistent brain-wide activation by blue, but not yellow stimulation ($p<0.05$, uncorrected, Supplementary Figure S2.a-b).

We next selected 28 regions of interest (ROIs) from the cortex and subcortical areas that are involved in reward and punishment, according to the Allen mouse brain atlas (Table 1, see Regions of interest in Methods), and extracted regional average beta values (regression coefficients) from the GLM. Comparison of regional beta values between the transgenic and wild-type groups revealed that the BOLD response was significantly higher in the transgenic group in 12 of 14 cortical regions, including OFC, mPFC and ACC, and 12 of 14 subcortical regions, including CPu, VTA, LHb, and DRN (Figure 2.b).

The week after session 1, we performed another session under the same stimulation parameters as in session 1. Patterns of BOLD responses were similar to those in session 1(transgenic: n = 7, WT: n = 6, Supplementary Figure S3). Pearson's correlation of the beta values in sessions 1 and 2 was r = 0.875, which was statistically significant ($p < 1e-8$; Supplementary Figure S7.a). The peak amplitude and peak timing of the BOLD responses varied across the 28 ROIs (Supplementary Figure S8.c-d), with the largest responses in the VTA, SNr and FP. Both the amplitude and timing of BOLD responses in sessions 1 and 2 were significantly correlated for blue light stimulation (amplitude: r = 0.886, $p < 1e-8$; timing: r=0.679, $p<0.005$), but not for yellow stimulation (amplitude: r = -0.06, p = 0.766; r = 0.037, p = 0.855; Supplementary Figure S8.a, b). These results indicate that our photo-stimulation of DRN induced consistent activation of DRN serotonergic neurons, which caused distinct spatial and temporal responses in multiple cortical and sub-cortical regions.

DRN Serotonin activation induces a brain-wide negative response in the BOLD signal under anesthesia

Contrary to our above results, a previous optogenetic fMRI study reported that DR serotonin activation evoked negative cortical cerebral blood volume (CBV) responses, an enhanced proxy of BOLD signals, from the entire cortical region under anesthesia [9]. There are two critical differences between the previous and current studies: the optogenetic probes and anesthesia. The previous study used the ePET-Cre mouse line and AAV harboring Cre-dependent ChR2 and applied 20-Hz photostimulation. On the other hand, the current study used Tph2-ChR2(C128S) transgenic mice, which express step-type opsin, to allow continuous activation by a pulse of blue light at the beginning and yellow light at the end (Figure 1e). Another difference is that the previous study employed isoflurane, a general gas anesthetic with a muscle relaxant, while our experiment employed no anesthetics.

In order to test the possibility that the difference is due to anesthesia, we compared BOLD responses to DRN serotonin stimulation between anesthetized and awake states in the same animals. We performed the same ON/OFF stimulation protocol under anesthesia with 1% isoflurane with the same groups (Transgenic: n = 6, WT:n = 5, Figure. 3.a). We also performed another ON/OFF stimulation session the next day in an awake state in order to eliminate possible confounding by diminished responses after repetitive photo-stimulation (Figure. 3.b).

Under anesthesia, we observed mostly negative BOLD responses from entire entire cortical region, while BOLD signals in the DRN remained positive (statistical $t > 1$, uncorrected; Figure. 3.a). On the other hand, session 4 under an awake state replicated positive BOLD signals from mid-line cortical regions and DRN (statistical $t > 1$, uncorrected; Figure. 3.b). We then contrasted regional beta values in anesthetized and awake states (Figure. 3.c). In the anesthetized state, multiple regions, such as ACC, dRSC, vRSC, DA and CA1 showed negative beta values, significantly different from those in the awake state ($p < 0.05$, correction of multiple comparisons with FDR). We further found a statistically significant difference in peaks of % BOLDs of these regions between anesthetized and awake states ($p<0.05$, Figure. 3.d; Supplementary Figure. S11). Our results support the hypothesis that general anesthesia induced negative BOLD responses by DR serotonin photo-activation.

Brain-wide BOLD responses are explained by serotonin projection density and receptor expression profiles

Our results revealed a brain-wide profile of evoked BOLD signals by DR serotonin activation (Figure. 2.a). One plausible mechanism underlying such a spatial profile is the density of the serotonergic projection pattern from DRN. In order to test such a possibility, we checked the correlation between intensity of projections of DRN serotonin neurons and the peak levels of BOLD responses. We extracted serotonin-specific structural projection density from DRN from the Allen Brain Atlas (Figure. 4.a.).

Serotonin projection density was statistically correlated with beta values under blue stimulation ($r = 0.491$, $p < 0.01$) but not under yellow stimulation ($r = 0.146$, $p = 0.481$; Figure 4.b.). We also found that projection density was significantly correlated with photo-stimulated BOLD responses in awake and anesthetized states (Anesthetized (Session3): $r = 0.546$, $p < 0.01$; Awake(Session4): $r = 0.758$, $p < 0.01$, FDR corrected; Figure. 4.c.).

We further investigated whether photo-stimulated BOLD responses are associated with serotonin synaptic receptors. Gene expression maps for 5-HT1A, 5-HT1B, 5-HT1F, 5-HT2A, and 5-HT2C receptors were obtained from the database of the Allen Brain Atlas (Supplementary Figure. S12). We then constructed a multiple linear model (MLM; Figure. 5.a) composed of one dependent variable of the BOLD response and six independent variables of the projection density and five gene expression patterns (5-HT1a, 5-HT1b, 5-HT1f, 5-HT2a, and 5-HT2c receptors) after normalization. The

model could reproduce the BOLD response with R2=0.66, showing statistical significance ($p < 0.01$). We also checked the consistency of the model using BOLD responses in different sessions. We found a significant correlation of the regression coefficients of session 1 with those in the awake state, but not in the anesthetized state (Anesthetized (Session3): $r = 0.373$, $p = 0.066$; Awake (Session4): $r = 0.655$, $p < 0.01$, FDR corrected; Figure. 5.b-c.).

We further investigated the contribution of each receptor by the estimated regression coefficients in the anesthetized and awake states (Figure. 5.d). In the awake state (Session 4), gene expression of 5-HT1 type receptors (5-HT1a, 5-HT1b, and 5-HT1f) showed negative coefficients, indicating negative contributions to BOLD responses. On the other hand, gene expression of 5-HT2 type receptors showed positive coefficients indicating positive contributions to the BOLD responses. In the anesthetized state (Session 3), negative weights for 5-HT1a and 5-HT1f receptors were more pronounced and the weight for 5-HT2c receptors was negative (also see Supplementary Figure. S14). This result implies that general anesthesia affects responses of 5HT receptors.

These results suggest that photo-activated BOLD responses reflect projection density of serotonin neurons and serotonin receptor expression profiles and that general anesthesia affects responses of 5-HT1 and 5-HT2 type receptors differently to induce altered BOLD responses.

Discussion

Our opto-fMRI investigation of the DRN serotonergic modulations of brain-wide dynamics brought three major discoveries. First, DRN serotonergic activation causes brain-wide positive BOLD responses in an awake state. Second, DRN serotonergic activation under general anesthesia causes brain-wide negative BOLD responses. Third, the whole-brain profile of DRN serotonin-activated BOLD signals is associated with the density of DRN serotonergic projection density and the expression profiles of 5-HT receptors, with opposite weights for 5-HT1 and 5-HT2 type receptors.

The present result of brain-wide activation by DRN serotonergic activation provides a reference for interpretation of recording and manipulation studies in humans and animals [5,12,17,22–25,32,35]. Previous studies have demonstrated serotonin's involvement in motivation and reward-related learning [3,22] through modulation of the ACC and ventromedial PFC on learning signals [32], CPu on short/long-term prediction of rewards

[35], and mPFC and OFC on waiting for delayed rewards [23]. Our opto-fMRI results support those studies, as those areas were consistently activated by DRN serotonin stimulation. In addition, average amplitudes of BOLD responses and peak timing are region-dependent. This finding implies that serotonin-activated BOLD responses are coupled with different regional distributions of receptor densities and serotonin projection, but not with the distance of the activation site. In spite of the indirect evidence, our linear approximation of serotonin-activated BOLD responses support such a possibility.

Serotonergic modulation in a short-term window using optogenetics can avoid the limitations in a long-term window, such as pharmacological manipulation [2,31,32] and chemogenetic manipulation with DREADD (designed receptors exclusively activated by designed drugs) [8]. Multiple pharmacological studies have applied SSRIs to manipulate the serotonin system. Systemic SSRI administration causes brain-wide inhibitory modulation [2,31]. However, the influence of SSRI administration on brain activity can be confounded by administration period due to receptor sensitivity [6,14,31].

A previous study stimulated the serotonin system with specifically designed drugs under fMRI [8] and revealed brain-wide positive responses in the somatosensory cortex and subcortical regions, including the hippocampus, the hypothalamus, and the cerebellum. The study did not reveal BOLD responses of mid-line cortical regions, such as the OFC, mPFC and ACC. A possible explanation for the difference between their results and ours is that BOLD responses cause different time scales, depending on receptor types. Our optogenetic fMRI approach revealed an influence on motivation-related regions at different timings in a transient time window (Supplementary Figure S5 and S8). Further studies will uncover neural mechanisms underlying different time scales of serotonin modulation via different methodological approaches, including optogenetics and chemogenetics.

The mechanism underlying different serotonin modulation between awake and anesthetized states remains unknown. One possible mechanism is a reduction of glutamate transmission via serotonin in target regions [36,37]. Previous studies revealed that isoflurane suppresses neural activity via inhibition of glutamatergic transmission [36,39]. We found that isoflurane reduced photo-stimulated BOLD signals where they were potentiated in an awake state. Our results also showed that some regions show potentiated negative BOLD responses. In addition to reduced glutamatergic transmission,

isoflurane also enhances sensitivity of GABA neurons [4,41]. Such higher responses of GABA neurons and lower responses of glutamatergic neurons may result in diminished positive BOLD signals and potentiated negative BOLD signals Future studies are needed to clarify the neural mechanism underlying BOLD signals under anesthesia.

We have also demonstrated that different types of 5-HT gene expression are associated with photo-activated BOLD responses. Distinctive contributions of serotonin receptor types influence neural activities mostly at metabotropic receptors [21]. 5-HT1 receptors are inhibitory metabotropic receptors to suppress neural activity by modulating the cellular signal cascade while 5-HT2 receptors are excitatory metabotropic receptors to activate neural activity [26,29]. Our MLM analysis revealed that regression coefficients of gene expression of 5-HT1 receptors and 5-HT2 receptors are negative and positive, respectively. The correspondence between functions of receptor types and signs of coefficients imply that BOLD responses by DRN serotonin photo-activation can be influenced by different receptor distributions. Nonetheless, how 5-HT receptors react distinctively to serotonin transmission under general anesthetics is unclear. Some studies revealed that isoflurane lessens spontaneous serotonin levels and spontaneous firing [19,38]. These changes of serotonin transmission may influence 5-HT receptors under anesthesia.

While our results replicated the negative cortical responses under anesthesia [9], it is worth mentioning three important differences in methodology and results between the previous and current studies. First, the previous study utilized cerebral blood volume (CBV) signals with a contrast agent to enhance influence of serotonin modulation, although the current study employed BOLD signals. Although CBV signal are an enhanced proxy of BOLD signals, the methodological difference in imaging may show different responses from various brain regions. Second, we employed the transgenic group targeting the tryptophan hydroxylase 2(Tph2) promoter [28,34] while the previous study employed the ePET-Cre line targeting transcription factor Pet1 [9]. While expression of ChR2 by the Tph2 promoter is highly selective for serotonergic neurons [25], the Pet1 promoter also causes expression in non-serotonergic neurons [16]. While CA1 and DG were significantly deactivated by serotonin photo-activation in our study, responses in the temporal regions were not found in the previous study [9]. Additionally, our results revealed an association between 5HT projection density and BOLD responses, but the previous study did not find this association. One critical methodological difference is that we employed different ROIs from those of the previous study. In the

current study, 28 ROIs from the Allen brain atlas, included other sources of serotonin and dopamine, MRN and VTA. In contrast, the previous study used 38 ROIs from the Australian Mouse Brain Mapping Consortium (AMBMC, https://www.imaging.org.au/AMBMC) with multiple ROI hippocampal formations and midbrain regions. The ROI difference may yield different results in the association between structural connectivity and responses by optogenetic serotonin activation. Further research is required to dissect the difference between two experimental results.

In conclusion, we reported brain-wide responses of DRN serotonin activation via opto-fMRI for the first time in awake animals. We found serotonergic modulation of widespread cortical and sub-cortical targets at different timing as a key controller of brain-wide information transmission. We also showed different modulation by the serotonin system in awake and anesthetized states. We also showed that serotonergic structural projections and gene expression profiles of 5-HT receptors are associated with BOLD responses. Further research is required to dissect complex serotonin modulation of brain-wide dynamics, given its neural and molecular mechanisms, such as interactions with neural population and receptors. Our findings provide a new physiological basis for understanding serotonergic control of brain-wide dynamics and functions.

Materials and Methods

All experimental procedures were performed under protocols accepted by the Okinawa Institute of Science and Technology Experimental Animal Committee.

Animals

Serotonin neuron-specific channelrhodopsin 2 variant(C128S) mice were generated by crossing Tph2-tTA mice with tetO-ChR(C128S)-EYFP knock-in mice under control of the tryptophan hydroxylase 2(Tph2) promoter [28,34]. Eight bi-genic and six wild-type (WT) C57BL/6J male mice (age > 12 w.o.) were used in this study. Mice were housed at 24 ◦C. on a inverted dark:light cycle (lights on 10:00-22:00, GMT+9). After stereotaxic surgery, mice underwent habituation training [42], MRI experiments, and a reward delay task in turn.

Stereotaxic surgery

Mice were initially sedated with 1-3% isoflurane, and were administered three types of mixed anesthetic agents (1 (mg/mL) of medetomidine, 5.0 (mg/mL) of midaloram, and 5.0 (mg/mL) of butorphanol, i.p.) [13]. The head skin was removed with a sterilized

surgical knife, and a plastic bar (3x3x27mm) for head-fixation in the MRI environment and an optic fiber (480 µm diameter, 4 mm length, Doric Lenses) was fixed to the skulls with dental acrylic cement. The optical fiber toward the DRN was horizontally implanted from the cerebellum in each of the mice. Mice were housed separately after surgery and underwent at least a 1-week recovery period. Mice were habituated to the MRI environment for at least another week. Mice subsequently underwent imaging sessions.

Acclimation

In order to habituate awake mice to the MRI imaging protocol, an acclimation protocol was applied to the mice after the surgeries for head-fixation [1,42]. Mice were fixed in a mock MRI environment and exposed to MRI imaging sounds and visual blue illumination for 2 h to habituate them to a leak of illumination during scanning (2.0 Hz). Acclimation to sounds and illumination was repeated 7 days prior to the first imaging session. Following imaging sessions, at least 3 days acclimation was permitted.

Functional magnetic resonance imaging (fMRI)

Each animal was placed in the MRI animal bed. T2-weighted structural imaging and three T2* functional imaging sessions were performed. MRI images were acquired with an 11.7-tesla MRI scanner for small animals (Biospec 117/11 system, Bruker Biospin, EmbH, Ettlingen, Germany) with a cryogenic quadrature RF surface probe (Cryoprobe, Bruker BioSpin AG, Fällanden, Switzerland). We performed T2-weighted structural imaging with a RARE sequence with subsequent parameters: 140 x 140 matrix, 13.5 x 13.5 mm2 field-of-view, repetition time(TR)/effective echo time(TE) 4000/18.75 (ms), 31 coronal slices, slice thickness: 300 µm.

After T2-weighted structural imaging was performed, a functional MRI session was further executed. A functional MRI session was composed of two imaging runs, a blue-yellow light stimulation run, and a yellow-light stimulation run. All functional imaging was performed using a GE-EPI sequence with following parameters: 67 x 67 matrix, 13.5 x 13.5 mm2 field-of-view, TR/TE 1000/10.7 (ms), flip angle: 50◦, bandwidth: 333k(Hz), 31 coronal slices and slice thickness: 300 µm, and 690 repetitions.

ON/OFF stimulation paradigm

A stimulation protocol was composed of ON/OFF stimulation patterns (Figure. 1.d). In each activation session, stimulation was initiated 90 volumes after the onset of an imaging session. DRN serotonin neurons were stimulated with blue illumination (490 nm,

3.0 mW, 1.0 sec), and stimulation subsequently ceased with yellow illumination (630 nm, 3.0 mW, 1.0 sec) 20 seconds after the onset of blue illumination. This stimulation was repeated 5 times for 120 seconds after the onset of blue illumination. For the control session, instead of blue illumination, only yellow illumination was applied in stimulation sessions.

Preprocessing and denoising

The first 10 volume images of each session were removed from subsequent analysis due to initial imaging instability caused by motion and non-steady state image quality. 10-fold magnification of images was done to process images with Statistical Parametric Mapping 12 (SPM12), which is designed to process human-size brain images. Therefore, the voxel size was 2 x 2 x 3 mm in analytical steps. Pre-processing, including motion correction, realignment, co-registration, normalization to a C57BL6/J template [11], and spatial smoothing (kernel with 3 x 3 x 6 mm) was executed with Statistical Parametric Mapping (SPM12). Since each slice of a 3D brain image was taken at a different time, slice timing correction was applied to correct slice-timing differences by temporal interpolation. Next, realignment of 3D brain images was conducted to correct motion-related changes of brain position. Then, co-registration was executed to overlay functional T2* images onto structural T2 images and to save coordination changes of T2* images for normalization. During normalization, T2 structural images were first warped to fit the average C57BL6/J template [11]. Then T2* functional images were further warped to the template using the co-registered coordination change of the images. In spatial smoothing, voxel signals were spatially smoothed using a gaussian kernel (4 x 4 x 6 mm). After pre-processing steps, the general linear model in SPM12 was executed to map spatial activation patterns.

Regions of Interest

The Allen brain institute provides a parcellation of the C57BL6 mouse brain. In order to extract BOLD signals from anatomically defined brain regions, this parcellation was utilized for subsequent analyses. Parcellation was first warped to the MRI template using Advanced Normalization Tools (ANTs), and 28 regions of interest (ROIs) were selected from the warped parcellation. 28 ROIs were selected with the following three criteria. First, primary cortical regions, especially mid-line regions, were selected. Second, primary reward- and punishment-related sub-cortical regions, including basal ganglia VTA, and DRN should were included. Third, ventro-lateral cortical and sub-cortical regions, such as the amygdala complex were not selected due to its sensitivity to artifacts near air cavities by the ear canals.

Activation map and BOLD responses

A general linear model (GLM) was performed to map beta values of parameter stimation of optogenetic stimulation onto the mouse brain template with SPM12. For statistical functional mapping of optogenetic stimulation, each voxel under an uncorrected P value ¡ 0.001 was thresholded, and cluster-wise multiple comparisons were subsequently executed with family-wise error (FWE) by thresholding pFWE < 0.05 with probabilistic threshold-free cluster enhancement (pTFCE) [33]. Statistical second-level voxel-wise analysis was finally executed to compare functional maps of transgenic mice to that of WT mice. Furthermore, regional beta values were extracted based on ROIs. Statistical significance of regional beta values were subsequently tested with Student's t tests with multiple comparisons with the false
discovery rate (FDR; pFDR < 0.05). Each regional BOLD signal change (%) is calculated by averaging regional time series on voxels, which are scaled with the mean of time series during the no-stimulation period and followed with multiplication by 100.

Structural density and RNA expression maps

The structural density map of serotonin connections was obtained from the mouse brain database of the Allen Brain Institute (Experimental IDs: 480074702) [10]. As with the structural density map, gene expression of serotonin receptors was obtained from the mouse brain database of Allen Brain Institute (Experimental IDs: 79556616 (5HT1a), 583 (5HT1b), 69859867 (5HT1f), 81671344 (5HT2a), and 73636098 (5HT2c)). Normalized energy intensity was extracted from the normalized atlas. Multiple linear model analysis of ROIs between betas from GLM analyses and gene expressions was performed.

A reward delay task

After imaging sessions, some mice from both groups (Transgenic: n=3, WT: n=2) subsequently performed a waiting experiment for a delayed reward. A sequential tone-food waiting task was utilized for a free operant task [24,25] (Supplementary Figure. S1.a). After MRI sessions, individual subjects were trained and tested in an operant-conditioning box (Med-Associates, 12.7x12.7 cm). In short, subjects were require to initiate trials by nose-poking into a tone site 500 (ms). The reward-delay task was composed of reward trials (75%) and omission trials (25%). We adopted two types of stimulation protocols (Supplementary Figure. 1.b): fixed-delay and random-delay protocols. At the onset of reward and omission trials, either blue or yellow illumination

was delivered. In the reward trials, blue/yellow light stimulation was delivered at the onset of each trial until nose-poking was performed, and yellow light was delivered when subjects waited for 6.0 (s) for the fixed protocol and 2, 6, or 10 (s) for the random delay protocol. However, yellow illumination was also given when subjects failed to wait for the delay. On the other hand, during omission trials, yellow stimulation was given when mice gave up waiting for delayed rewards while light stimulation was delivered in the same manner as in the reward trials.

Data and code availability

Raw data including functional and structural images will be available soon. Codes and pre-processed data are also available from https://github.com/Taiyou/OptofMRI5HT. All software used in this study is also available (Supplementary Table. S2)

Acknowledgments

We acknowledge Dr. Toda (Keio Univ.) for his comments on awake optogenetic stimulation, Dr. Hikishima for his comments on fMRI, Mr. Ohba for creation of acclimation tools, and DMD. Jiafu Zeng for animal support for MRI acquisition.

Author contributions statement HTH and KD conceived the experiments. HTH, AY, NT designed and prepared experiments, HTH performed MRI experiments. MT conducted behavioral experiments. HTH analysed results, and HTH wrote the manuscript. All authors reviewed the manuscript.

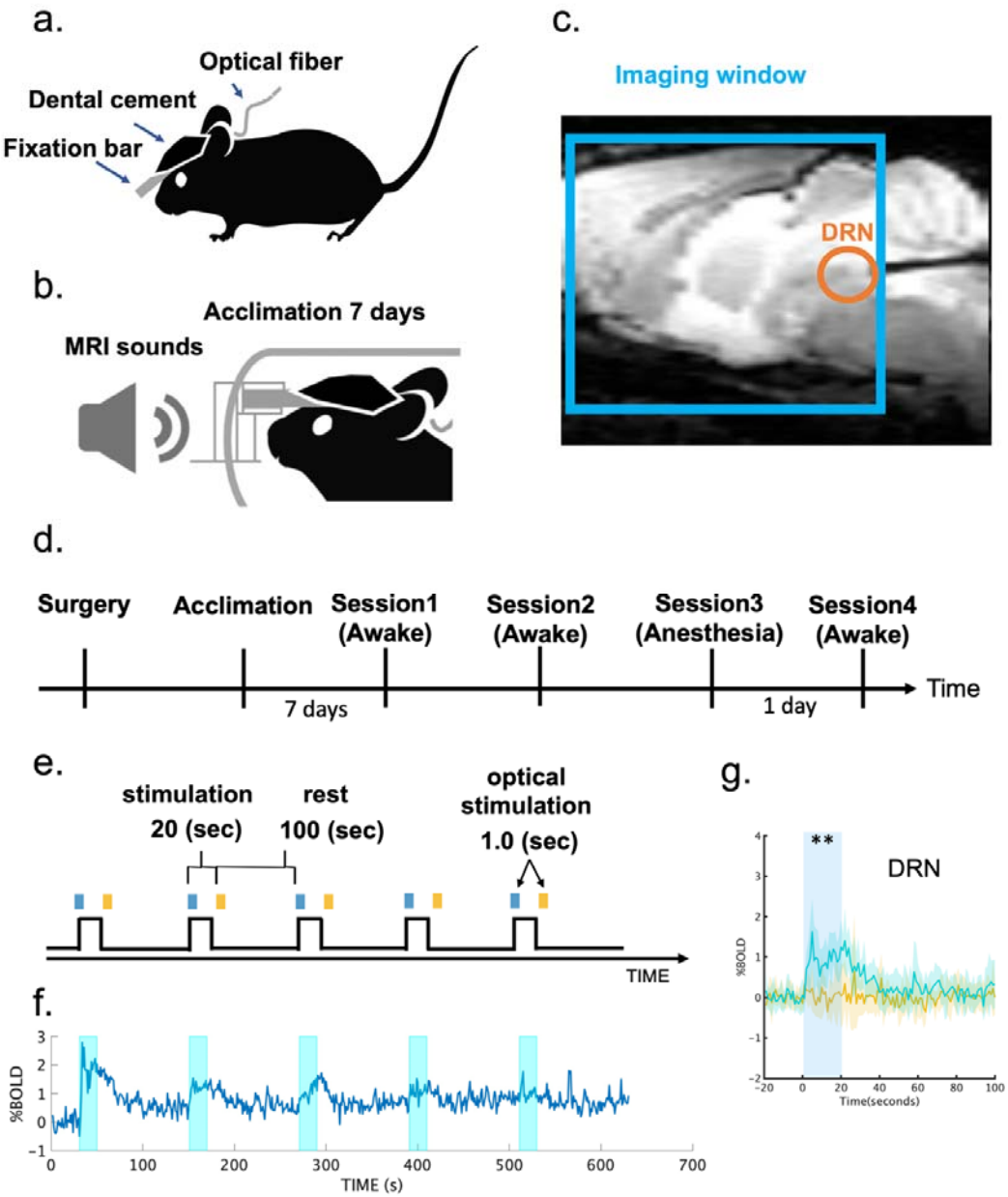

Figure 1. (a) Surgerical setup. A fixation bar was mounted on the mouse head with dental cement and an optical cannula was inserted into the dorsal raphe nucleus (DRN) (b) Acclimation protocol. A mouse was exposed daily to recorded MRI scanning sounds for 2 h for 7 days prior to fMRI sessions. (c) Location of an optical cannula. An optical cannula was horizontally inserted into the DRN from the cerebellum. A cyan window indicates the imaging window for T2* sessions. (d) Experimental schedule. After surgery and 7 days acclimation, the first fMRI recording session was performed. A replication session was also performed a few weeks later. Finally, experiments for anesthesia effects were performed. On the 1st day, an fMRI recording with general anesthesia by isoflurane 1% was performed, and an fMRI recording

without anesthesia was conducted thereafter. (e) Stimulation protocol. In an fMRI session, the onset of optogenetic stimulation was applied 90 s after an imaging session began. Blue illumination (1.0 s; 473 *nm*) was applied and yellow illumination (1.0 second; 593 *nm*) followed 20 s after blue illumination. (f) Average time course of % BOLD signals in DRN. Time series of % BOLD signals were individually extracted from DRN in session 1 and session 2, and the time series were averaged across transgenic mice (n = 8). (g) Alignment of average % BOLD responses in DRN. % BOLD responses were aligned at the time of blue illumination in session 1. Blue and yellow lines indicate % BOLD responses in DRN from blue and yellow stimulation sessions from the transgenic group (n = 8), respectively.

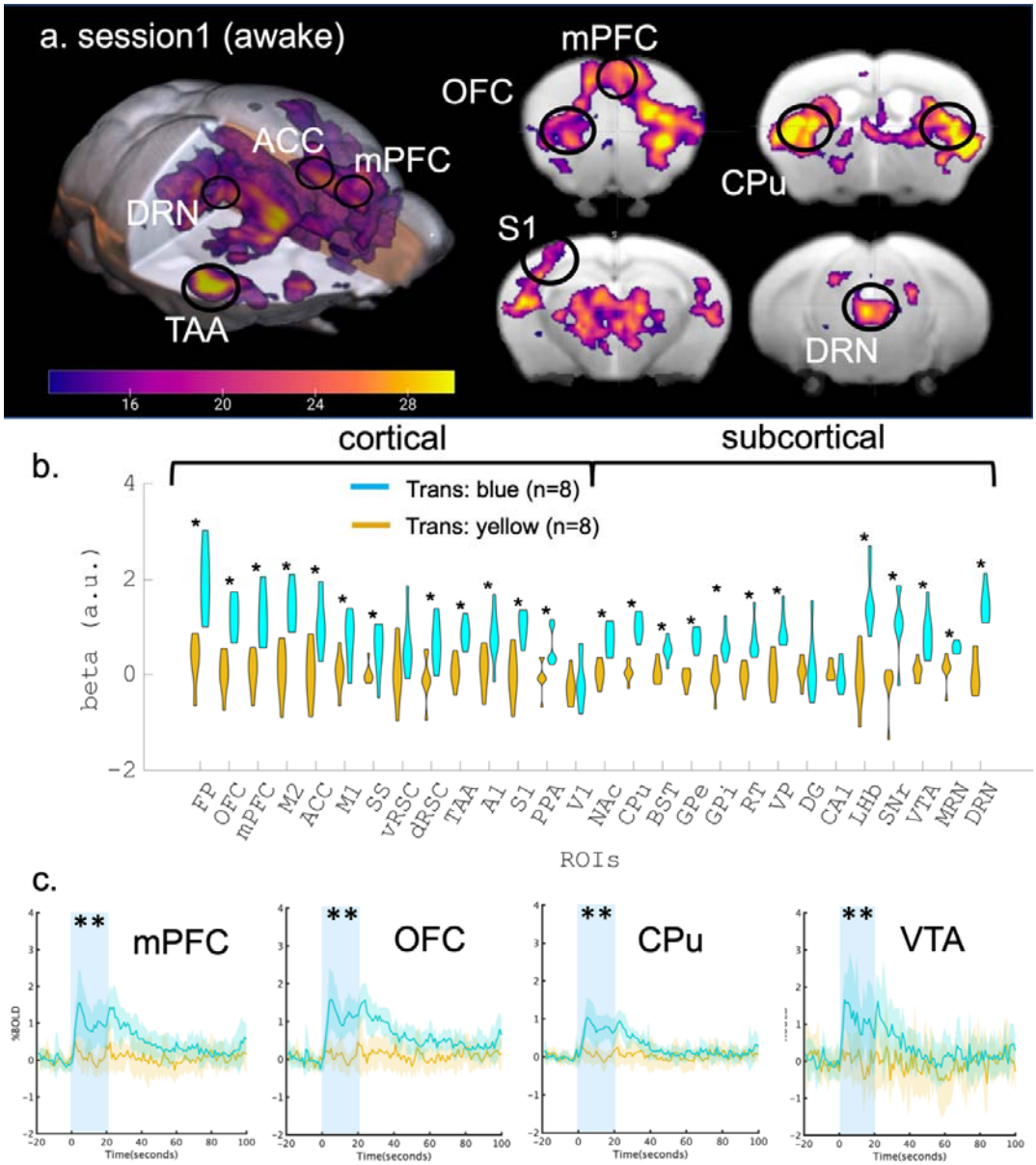

Figure 2. (a) Functional map of optogenetic illumination. A functional map was calculated by contrasting BOLD responses between the blue and yellow illumination in the transgenic (n = 8) group ($p < 0.05$, cluster-corrected). Magenta color indicates statistical t value. (b) Comparison of beta values in multiple ROIs. Beta values were obtained from GLM analysis in session 1, and were extracted and averaged based on ROIs from the Allen Brain Atlas (Table 1). The difference of beta values between blue and yellow illumination sessions were contrasted in the transgenic group. * indicates $p<0.05$ (multiple comparison was corrected with false discovery rate (FDR)). Cyan and magenta colors indicate blue and yellow illumination, respectively. (c) Alignment of average % BOLD responses in mPFC, OFC, CPu, and VTA. % BOLD responses were aligned at the time of blue illumination in session 1. Blue and red lines

indicate % BOLD responses in mPFC, OFC, CPu, and VTA from transgenic (n = 8) and WT (n = 6) groups, respectively. A cyan window indicates stimulation duration during a session for 20 s.

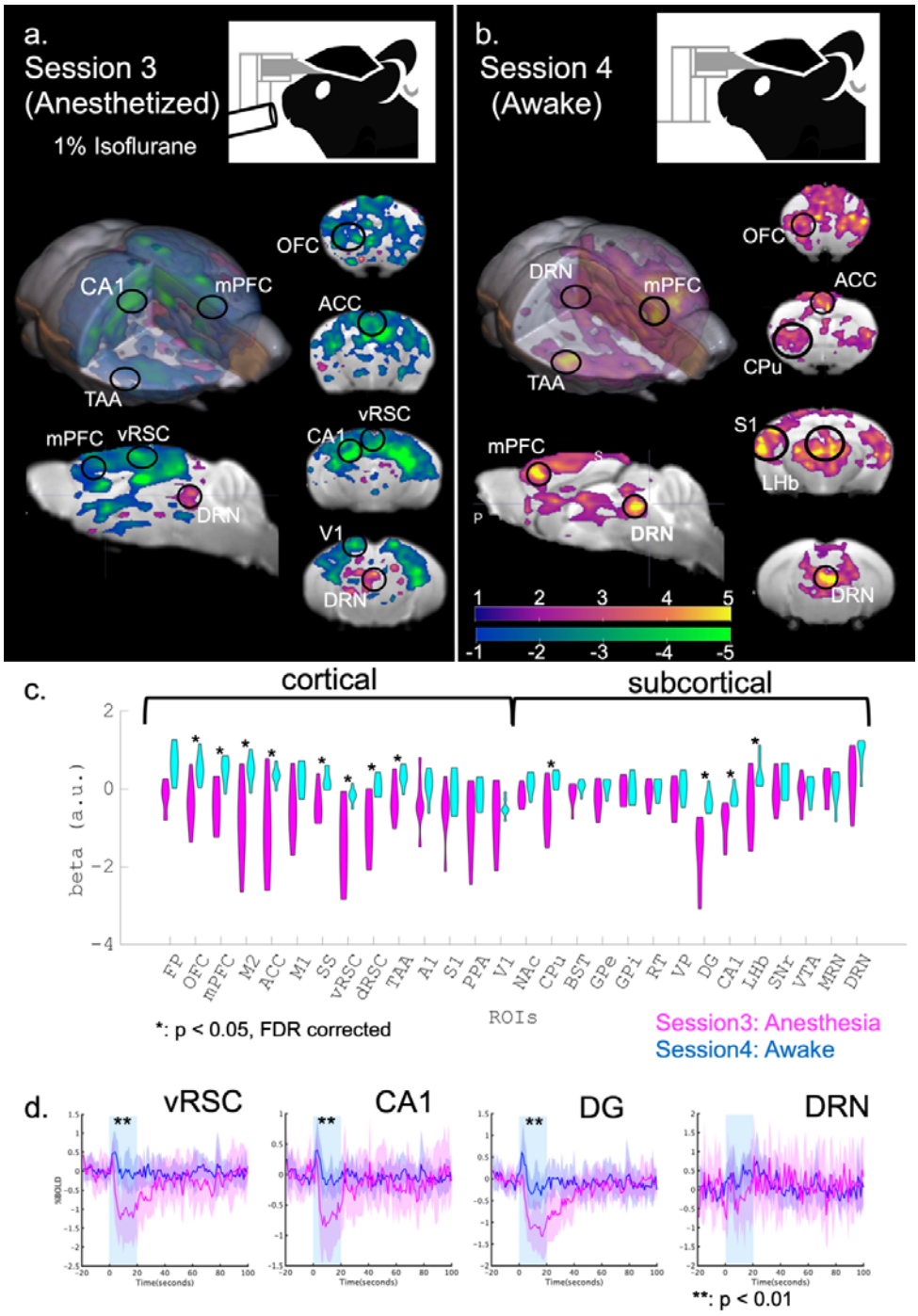

Figure 3. (a) Optogenetic fMRI session with general anesthesia in session 3. General anesthesia, 1% isoflurane, was applied to transgenic and WT groups during optogenetic fMRI sessions. GLM analysis following optogenetic stimulation was executed and visualized (t > 1, uncorrected). Magenta and cyan colors indicate positive and negative statistical t values. (b) Optogenetic fMRI session under the awake state in session 4. As in session 1, no anesthesia was applied to transgenic and WT groups during

optogenetic fMRI sessions. As on day 1, GLM analysis was executed and visualized ($t > 1$, uncorrected). (c) Comparison between beta values of sessions 3 and 4 in multiple ROIs. Beta values of blue illumination sessions in session 3 and session 4 were statistically contrasted using Student's t test. * indicates $p<0.05$, FDR-corrected). (d) Alignment of average % BOLD responses in vRSC, CA1, DG, and DRN in session 3 from transgenic mice. A cyan window indicates stimulation duration during a blue illumination session for 20 seconds. ** indicates $p<0.05$.

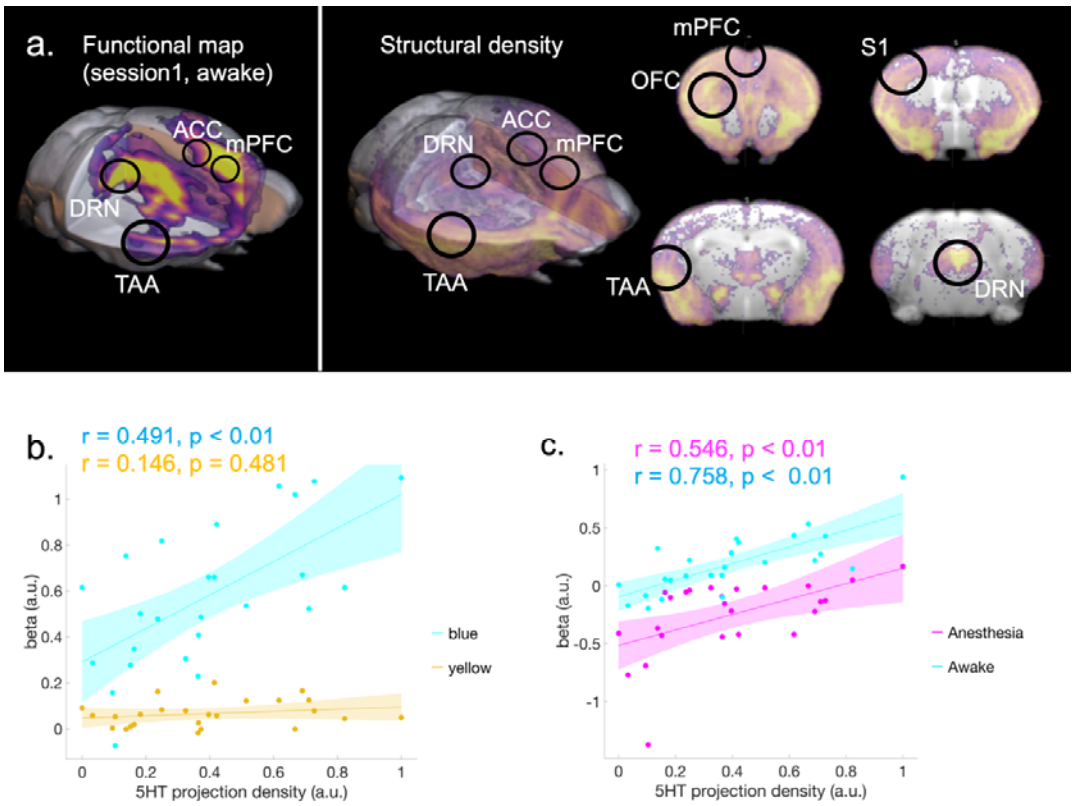

Figure 4. (a) Structural density map of serotonergic projection. A structural density map of serotonergic projections was obtained from the Allen brain atlas. (b) Correlation between projection density and regional beta values. The correlation between regional structural density and average regional beta values across transgenic groups was calculated from session 1. Blue and yellow colors indicate data from blue and yellow illumination sessions, respectively. (c) Correlation between projection density and regional beta values. The correlation between regional structural density and average regional beta values across transgenic groups was calculated. Blue and orange colors indicate data from blue illumination sessions in sessions 3 and 4, respectively.

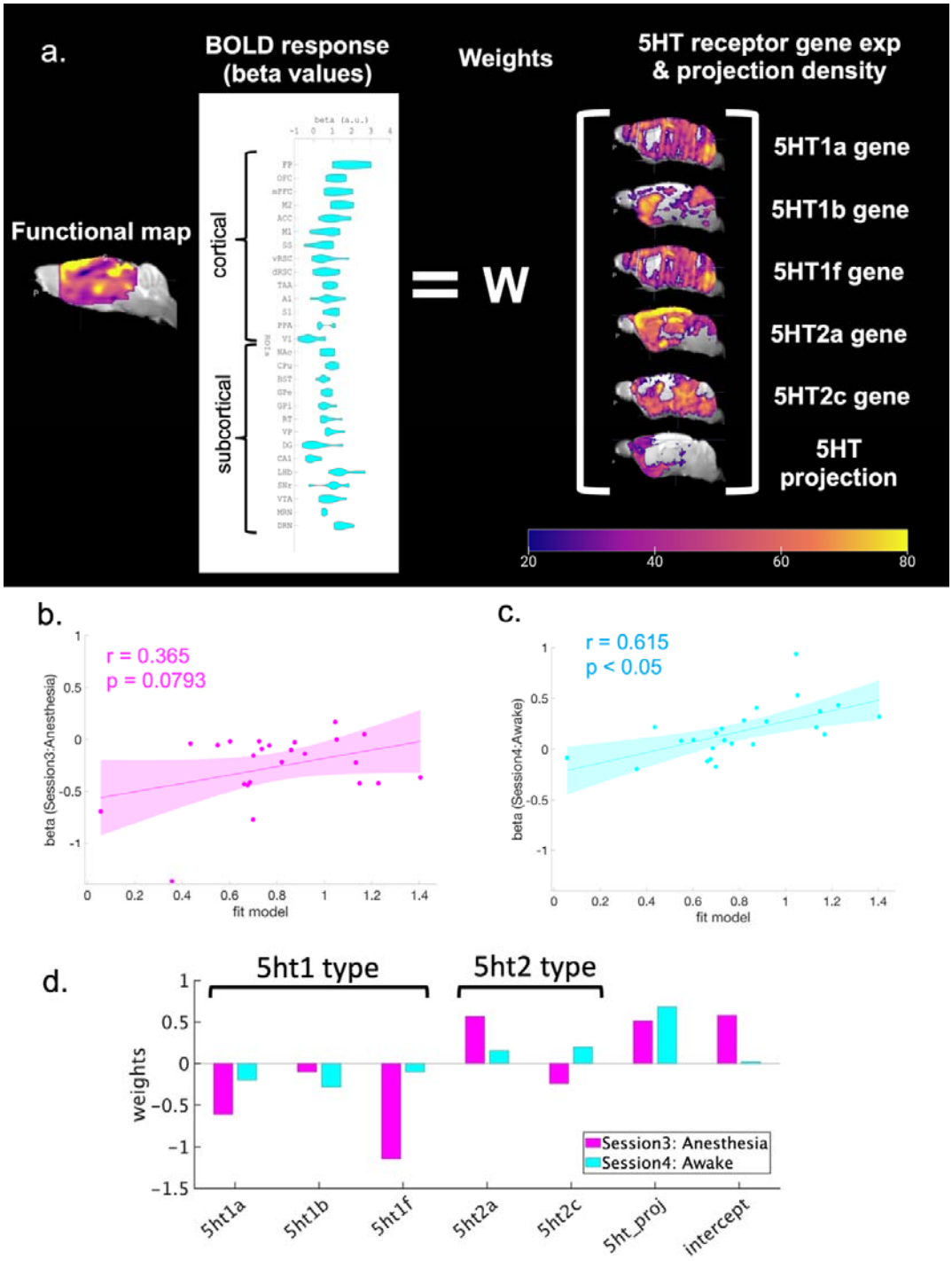

Figure 5. (a) Procedure to make a model of prediction of beta values in session 1 of blue illumination. Independent variables, including regional structural densities and regional gene expression of 5ht1a, 5ht1b, 5ht1f, 5ht2a, and 5ht2c were fit with a linear regression model to beta values of multiple ROIs from blue illumination sessions. (b) Correlation between modeled beta values from session 1 and beta values from

session 3 under anesthesia. (c) Correlation between modeled beta values from session 1 and beta values from session 4. (d) Weights from the fit models with session 3 under anesthesia and session 4 without anesthesia. Magenta and cyan colors indicate weights of expression profiles from session 3 and session 4, respectively.

References

1. Abe Y., Takata N., Sakai Y., Hamada H. T., Hiraoka Y., Aida T., Tanaka K., Bihan D. L., Doya K., and K. F. Tanaka. Diffusion functional MRI reveals global brain network functional abnormalities driven by targeted local activity in a neuropsychiatric disease mouse model. *Neuroimage*, 223:117318, 2020.

2. Anderson I. M., McKie S., Elliott R., Williams S. R., and Deakin, J. F. Assessing human 5-HT function in vivo with pharmacoMRI. *Neuropharmacology*, 55(6):1029–37, 2008.

3. Boureau, Y. L., and Dayan, P. Opponency revisited: competition and cooperation between dopamine and serotonin. *Neuropsychopharmacology*, 36(1):74–97, 2011.

4. Caraiscos V. B., Newell J.G., You-Ten K. E., Elliott E. M., Rosahl T. W., Wafford K. A., MacDonald J.F., and Orser B. A. Selective enhancement of tonic GABAergic inhibition in murine hippocampal neurons by low concentrations of the volatile anesthetic isoflurane. *J Neurosci*, 24(39):8454–8, 2004.

5. Fonseca M.S., Murakami M., and Mainen Z. F.. Activation of dorsal raphe serotonergic neurons promotes waiting but is not reinforcing. *Curr Biol*, 25(3):306–315, 2015.

6. Fritze S., Spanagel R., and Noori H.R. Adaptive dynamics of the 5-HT systems following chronic administration of selective serotonin reuptake inhibitors: a meta-analysis. *J Neurochem*, 142(5):747–755, 2017.

7. Fu W., Le Maitre E., Fabre V., Bernard J. F., David Xu Z. Q., and Hokfelt T. Chemical neuroanatomy of the dorsal raphe nucleus and adjacent structures of the mouse brain. *J Comp Neurol*, 518(17):3464–94, 2010.

8. Giorgi A., Migliarini S., Galbusera A., Maddaloni G., Mereu M., Margiani G., et al., Brain-wide mapping of endogenous serotonergic transmission via chemogenetic fMRI. *Cell Rep*, 21(4):910–918, 2017.

9. Grandjean J., Corcoba A., Kahn M.C., Upton A.L., Deneris E.S., Seifritz E., et al. A brain-wide functional map of the serotonergic responses to acute stress and fluoxetine. *Nat Commun*, 10(1):350, 2019.

10. Harris J. A., Hirokawa K.E., Sorensen S.A., Gu H., Mills M., Ng L.L., et al., Anatomical characterization of Cre driver mice for neural circuit mapping and manipulation. *Front Neural Circuits*, 8:76, 2014.

11. Hikishima K., Komaki Y., Seki F., Ohnishi Y., Okano H.J., and Okano H. In vivo microscopic voxel-based morphometry with a brain template to characterize strain-specific structures in the mouse brain. *Sci Rep*, 7(1):85, 2017.

12. Iigaya K., Fonseca M.S., Murakami M., Mainen Z.F., and Dayan P. An effect of serotonergic stimulation on learning rates for rewards apparent after long intertrial intervals. *Nat Commun*, 9(1):2477, 2018.

13. Kawai S., Takagi Y., Kaneko S., and Kurosawa T. Effect of three types of mixed anesthetic agents alternate to ketamine in mice. *Exp Anim*, 60(5):481–7, 2011.

14. Klomp A., Tremoleda J.L., Wylezinska M, Nederveen A.J., Feenstra M., Gsell W., et al., Lasting effects of chronic fluoxetine treatment on the late developing rat brain: age-dependent changes in the serotonergic neurotransmitter system assessed by pharmacological MRI. *Neuroimage*, 59(1):218–26, 2012.

15. Li Y., Zhong W., Wang D., Feng Q., Liu Z., Zhou J., et al., Serotonin neurons in the dorsal raphe nucleus encode reward signals. *Nat Commun*, 7:10503, 2016.

16. Liu Z., Zhou J., Li Y, Hu F., Lu Y., Ma M., et al., Dorsal raphe neurons signal reward through 5-ht and glutamate. *Neuron*, 81(6):1360–1374, 2014.

17. Lottem E., Banerjee D., Vertechi P., Sarra D., Lohuis M.O., and Mainen Z.F. Activation of serotonin neurons promotes active persistence in a probabilistic foraging task. *Nat Commun*, 9(1):1000, 2018.

18. Marcinkiewcz C.A., Mazzone C.M., D'Agostino G., Halladay L.R., Hardaway J. A., DiBerto J.F., et al., Serotonin engages an anxiety and fear-promoting circuit in the extended amygdala. *Nature*, 537(7618):97–101, 2016.

19. Massey C.A., Iceman K.E., Johansen S.L., Wu Y., Harris M.B., and Richerson G.B. Isoflurane abolishes spontaneous firing of serotonin neurons and masks their pH/CO(2) chemosensitivity. *J Neurophysiol*, 113(7):2879–88, 2015.

20. Matias S., Lottem E., Dugue G.P., and Mainen Z. F. Activity patterns of serotonin neurons underlying cognitive flexibility. *Elife*, 6, 2017.

21. Mengod G., Vilaro M.T., Raurich A., Lopez-Gimenez J. F., Cortes R., and Palacios J.M. 5-HT receptors in mammalian brain: receptor autoradiography and in situ hybridization studies of new ligands and newly identified receptors. *Histochem J*, 28(11):747–58, 1996.

22. Meyniel F., Goodwin G.M., Deakin J. W., Klinge C., MacFadyen C., Milligan H., et al., A specific role for serotonin in overcoming effort cost. *Elife*, 5, 2016.

23. Miyazaki K., Miyazaki K.W., Sivori G., Yamanaka A., Tanaka K.F., and Doya K. Serotonergic projections to the orbitofrontal and medial prefrontal cortices differentially modulate waiting for future rewards. *Sci Adv*, 6(48), 2020.

24. Miyazaki K., Miyazaki K.W., Yamanaka A., Tokuda T., Tanaka K.F., and Doya K. Reward probability and timing uncertainty alter the effect of dorsal raphe serotonin neurons on patience. *Nat Commun*, 9(1):2048, 2018.

25. Miyazaki K.W., Miyazaki K., Tanaka K.F., Yamanaka A., Takahashi A., Tabuchi S., et al., Optogenetic activation of dorsal raphe serotonin neurons enhances patience for future rewards. *Curr Biol*, 24(17):2033–40, 2014.

26. Nichols D.E. and Nichols C.D. Serotonin receptors. *Chem Rev*, 108(5):1614–41, 2008.

27. Ohmura Y., Iwami K., Chowdhury S., Sasamori H., Sugiura C., Bouchekioua Y., et al., Disruption of model-based decision making by silencing of serotonin neurons in the dorsal raphe nucleus. *Curr Biol*, 31(11):2446–2454 e5, 2021.

28. Ohmura Y., Tanaka K.F., Tsunematsu T., Yamanaka A., and Yoshioka M. Optogenetic activation of serotonergic neurons enhances anxiety-like behaviour in mice. *Int J Neuropsychopharmacol*, 17(11):1777–83, 2014.

29. Pytliak M., Vargova V., Mechirova V., and Felsoci M. Serotonin receptors - from molecular biology to clinical applications. *Physiol Res*, 60(1):15–25, 2011.

30. Ren J., Isakova A., Friedmann D., Zeng J., Grutzner S.M., Pun A., et al., Single-cell transcriptomes and whole-brain projections of serotonin neurons in the mouse dorsal and median raphe nuclei. *Elife*, 8, 2019.

31. Schaefer A., Burmann I., Regenthal R., Arelin K., Barth C., Pampel A., et al., Serotonergic modulation of intrinsic functional connectivity. *Curr Biol*, 24(19):2314–8, 2014.

32. Scholl J., Kolling N., Nelissen N., Browning M., Rushworth M.F., and Harmer C.J. Beyond negative valence: 2-week administration of a serotonergic antidepressant enhances both reward and effort learning signals. *PLoS Biol*, 15(2):e2000756, 2017.

33. Spisák T., Spisák Z., Zunhammer M., Bingel U., Smith S., Nichols T., et al., Probabilistic TFCE: A generalized combination of cluster size and voxel intensity to increase statistical power. *NeuroImage*, 185:12–26, 2019.

34. Tanaka K.F., Matsui K., Sasaki T., Sano H., Sugio S., Fan K., et al., A. Expanding the repertoire of optogenetically targeted cells with an enhanced gene expression system. *Cell Rep*, 2(2):397–406, 2012.

35. Tanaka S.C., Schweighofer N., Asahi S., Shishida K., Okamoto Y., Yamawaki S., et al., Serotonin differentially regulates short- and long-term prediction of rewards in the ventral and dorsal striatum. *PLoS One*, 2(12):e1333, 2007.

36. Wang H.Y., Eguchi K., Yamashita T., and Takahashi T. Frequency-dependent block of excitatory neurotransmission by isoflurane via dual presynaptic mechanisms. *J Neurosci*, 40(21):4103–4115, 2020.

37. Whittington R.A. and Virag L. Isoflurane decreases extracellular serotonin in the mouse hippocampus. *Anesth Analg*, 103(1):92–8, table of contents, 2006.

38. Whittington R.A. and Virag L. Isoflurane decreases extracellular serotonin in the mouse hippocampus. *Anesth Analg*, 103(1):92–8, table of contents, 2006.

39. Winegar B.D. and MacIver M.B. Isoflurane depresses hippocampal ca1 glutamate nerve terminals without inhibiting fiber volleys. *BMC Neurosci*, 7:5, 2006.

40. Xu S., Das G., Hueske E., and Tonegawa S. Dorsal raphe serotonergic neurons control intertemporal choice under trade-off. *Curr Biol*, 27(20):3111–3119 e3, 2017.

41. Ying S.W., Werner D.F., Homanics G.E., Harrison N.L., and Goldstein P.A. Isoflurane modulates excitability in the mouse thalamus via GABA-dependent and GABA-independent mechanisms. *Neuropharmacology*, 56(2):438–47, 2009.

42. Yoshida K., Mimura Y., Ishihara R., Nishida H., Komaki Y., Minakuchi T., et al., Physiological effects of a habituation procedure for functional MRI in awake mice using a cryogenic radiofrequency probe. *J Neurosci Methods*, 274:38–48, 2016.